Available online at www.sciencedirect.com
ScienceDirect
Journal of Power Sources 165 (2007) 324–336
JOURNAL OF POWER SOURCES
www.elsevier.com/locate/jpowsour

Measured effects of filling time and initial mass on the temperature distribution within a hydrogen cylinder during refuelling

C.J.B. Dicken [a], W. Mérida [a,b,*]

[a] *Clean Energy Research Centre, University of British Columbia, Vancouver, BC, Canada V6T 1Z4*
[b] *Institute for Fuel Cell Innovation, 4250 Wesbrook Mall, Vancouver, BC, Canada V6T 1W5*

Received 14 October 2006; received in revised form 9 November 2006; accepted 18 November 2006
Available online 12 January 2007

Abstract

We have measured the effects of the initial mass and the total fill time on the temperature rise and the temperature distribution within a compressed hydrogen cylinder during refuelling.

A type 3, 74 L hydrogen cylinder was instrumented internally with 63 thermocouples distributed along the mid vertical plane. The experimental fills were performed from initial pressures of 50, 75, 100, 150, and 200 bar at gas delivery rates corresponding to nominal fill times of 1, 3, and 6 min. The experimental conditions with larger ratios of final to initial mass produced larger temperature changes. However, the lower ratios generated the largest rates of temperature rise. Longer fill times produced lower final average gas temperatures (compared to shorter fills), and a temperature field with significant vertical stratification due to buoyancy forces at lower gas inlet velocities. A sensor located at the end opposite to the gas inlet could be suitable for fuel metering via temperature and pressure measurements only.

Keywords: Compressed gas cylinder; Hydrogen refuelling; Temperature distribution

1. Introduction

Compressed gas cylinders represent the simplest and most mature technology for hydrogen storage. They are also the preferred near-term option for direct-hydrogen and hybrid fuel cell vehicles. Although various shapes have been explored, the onboard tank is usually cylindrical, and it can be classified by the choice of structural materials. Types 3 and 4 cylinders are the cylinders of choice for vehicular applications because they provide the greatest volumetric and gravimetric storage densities (see Table 1). The liner in a type 3 or 4 cylinder provides a gas tight seal while the wrap (usually a carbon fibre) provides the structural integrity.

Refuelling vehicle cylinders involves transferring high-pressure hydrogen gas from the fuelling station tanks through a dispenser into the vehicle cylinder. The dispenser controls the rate of filling, ensures safe operation, and delivers the rated mass of gas. The total time required to refuel a cylinder (t_{total}) is important for consumer acceptance and it can have significant financial consequences in commercial applications. In central refuelling applications (transit buses, lift trucks, etc.), the refuelling time increases with fleet size. Current regulation imposes limits on the maximum average gas temperature allowed within the cylinder, and these limits also affect refuelling time. The current standards governing the use of cylinders for vehicular applications state that the average hydrogen temperature cannot exceed 358 K [1]. However, during refuelling there is a significant rise in temperature as a result of two phenomena described in greater detail in Section 2.

The choices for metering high-pressure hydrogen are limited. Coriolis meters, sonic nozzle meters and turbine meters have been considered. The meters currently used in natural gas fuelling stations contribute a significant portion to the cost of the entire dispenser. The most accurate and currently best-suited meter for high-pressure applications is the coriolis flow meter. Depending on the flow ranges, these units can cost in excess of $10,000. Metering the dispensed gas via temperature and pressure measurements can enable more economical dispensers.

* Corresponding author. Permanent address: Clean Energy Research Centre, University of British Columbia, 6250 Applied Science Lane, Vancouver, BC, Canada V6T 1Z4. Tel.: +1 604 822 4189; fax: +1 604 822 2403.
E-mail address: walter.merida@ubc.ca (W. Mérida).

0378-7753/$ – see front matter © 2007 Elsevier B.V. All rights reserved.
doi:10.1016/j.jpowsour.2006.11.077

Nomenclature

a	Redlich–Kwong constant for hydrogen
A	curve fitting coefficient
A_k	area element for thermocouple (m^2)
b	Redlich–Kwong constant for hydrogen ($m^3\ mol^{-1}$)
B	curve fitting coefficient
C	curve fitting coefficient
C_p	specific heat at constant pressure ($J\ mol^{-1}\ K^{-1}$)
C_v	specific heat at constant volume ($J\ mol^{-1}\ K^{-1}$)
h_{in}	specific enthalpy ($J\ mol^{-1}$)
H_j	sensor subset for horizontal temperature planes ($j = 0, \pm 1$)
L	cylinder length (m)
m	mass of gas inside the cylinder (kg)
$\dot{m}$	mass flow rate ($kg\ s^{-1}$)
m_f	final mass of hydrogen in the cylinder at the end of fill (kg)
m_i	initial mass of hydrogen present in the cylinder (kg)
P	pressure (bar)
P_i	initial pressure inside the cylinder (bar)
$\dot{Q}$	heat transfer rate (W)
R	cylinder radius (m)
R_{gas}	universal gas constant ($J\ mol^{-1}\ K^{-1}$)
t	time (s)
t_{total}	total time of the fill (s)
T	temperature (K)
T_i	initial temperature inside the cylinder (K)
T_{in}	temperature of inlet gas (K)
T_k	temperature measured by thermocouple k (K)
T_{mean}	volumetric mean temperature (K)
u	specific internal energy ($J\ mol^{-1}$)
U	internal energy (J)
v_{in}	specific volume of inlet gas ($m^3\ mol^{-1}$)
V	internal volume of the cylinder (m^3)
V_i	sensor subset for vertical temperature planes ($i = 1, 2, 3$)
x	distance from cylinder inlet (m)
y	vertical distance from cylinder axis (m)
y_k	radial distance to thermocouple k (K)

There have been many experimental studies of the temperature rise within a compressed gas cylinder during refuelling [2–10], but only a few have placed more than one temperature sensor within the cylinder to measure gas temperature. The only study that has placed enough temperature sensors within the vessel to provide a temperature distribution is the study of Haque et al. [4,8]. This study analyzed the blowdown of a large, cylindrical, steel pressure vessel. While insight was gained into experimental techniques, these results are not directly useful for the analysis of the temperature distribution within a type 3 cylinder (due to different materials and experimental conditions). Researchers at the Gas Technology Institute [5] also found a significant spatial variability in temperature. Three thermocouples located at 1/4, 1/2 and 3/4 lengths of the centerline all read significantly different temperatures during filling. Towards the end of filling the thermocouples at 1/4 and 3/4 lengths converged to single temperature while the thermocouple at 1/2 length took greater than 20 min to converge to the same reading.

Table 1
The performance factors for different cylinder types (adapted from Ref. [1])

Cylinder type	Description	Performance factor (inches)
Type 1	All steel tank	150,000
Type 3	Aluminum liner with carbon fiber wrap	1,300,000
Type 4	Plastic liner with carbon fiber wrap	1,250,000

Cylinder performance factor is defined as burst pressure multiplied by volume, and divided by weight.

Our objectives in the present study were: (i) to monitor and record the temperature field within a type 3 compressed gas cylinders during refuelling, (ii) to determine the effect of fill rate and initial pressure on the temperature field, and (iii) to determine the relationship between the temperature rise and the amount of gas dispensed during a fill.

To achieve these objectives this investigation was separated into three experimental phases. The first, determined the repeatability of the fill conditions and the experimental measurements of temperature and pressure. The second investigated the effects of fill rate, and the third initial pressure on the temperature field within the cylinder, respectively. The experiments were performed at the Pacific Spirit Hydrogen Fuelling Station located at the National Research Council's Institute for Fuel Cell Innovation in Vancouver, Canada.

These measurements have been used to validate numerical models and are being used to identify optimal placement of a single commercial sensor to approximate the average gas temperature (as measured from an experimental sensor grid). In collaboration with our industrial partners, the data gathered in this study will also be used to elucidate the heat transfer characteristics between the cylinder materials and the hydrogen fuel.

2. Theory

The thermodynamics of filling compressed gas cylinders has been the subject of most of the fast fill studies to date [2,4,6,7]. During refuelling there is a significant increase in gas temperature due to two combined phenomena.

For hydrogen the Joule–Thomson coefficient is negative at the temperatures and pressures of filling. As a result, an isenthalpic expansion of the gas from the high-pressure tank through the dispenser throttling device and into the low-pressure cylinder results in an increase in gas temperature. The isenthalpic expansion occurs within the dispenser and the gas entering the cylinder is thus preheated.

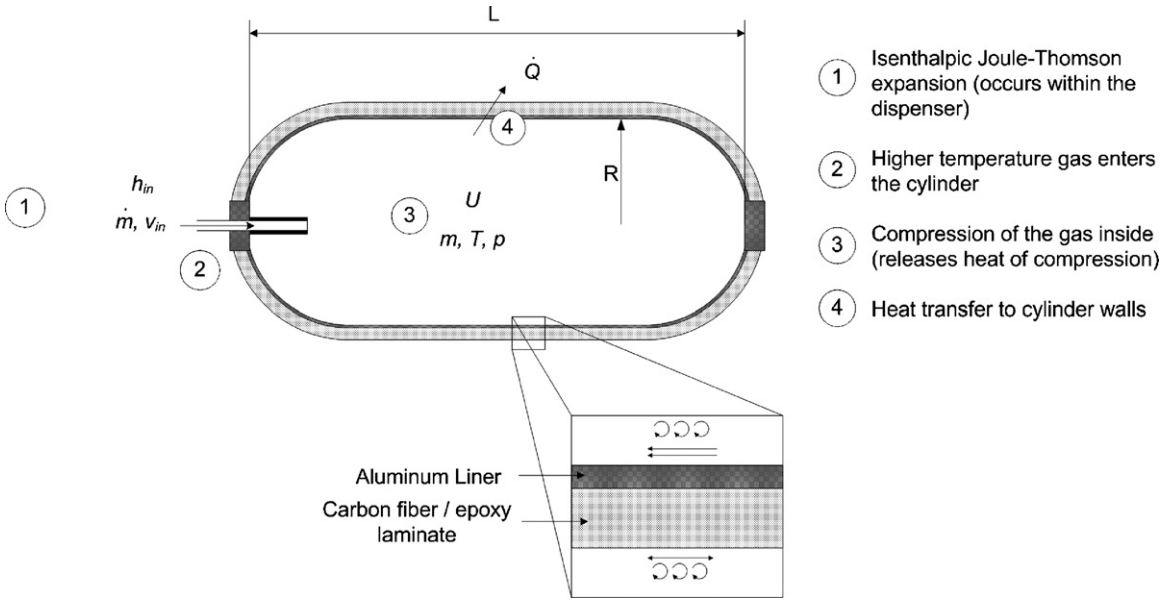

Fig. 1. Schematic of the filling setup for a compressed gas cylinder.

The second phenomenon that causes a temperature rise during filling is the compression of the gas inside the cylinder by the introduction of the higher-pressure gas from the fuelling station. This compression continues throughout the fill and the corresponding increase in temperature is known as the heat of compression. A comparison of the magnitudes of these two phenomenon shows that the Joule–Thomson effect has an insignificant effect on the overall temperature rise when consideration is given to the thermodynamics of the entire process. Overall, larger dispensing rates (in $\mathrm{kg\,s^{-1}}$) lead to larger heating rates (in $\mathrm{K\,s^{-1}}$) that affect the accuracy of the fill. When the temperature reaches the maximum limit (358 K) the gas delivery is halted independently of the final mass dispensed. As the gas cools, the pressure inside the cylinder decreases and this leads to well known under-filling issues on board fuel cell vehicles.

A simplified analysis of the filling of a compressed gas cylinder can be performed by treating the interior of the cylinder as a single control volume. Fig. 1 shows the layout of a typical cylinder with gas entering the cylinder from an inlet at one end of the cylinder. The compression of the gas within the cylinder yields a dramatic temperature rise, which is mitigated by heat loss from the gas to the cylinder liner. Part of the heat transferred to the liner is stored within the material and part is conducted through the cylinder wall to the environment.

A single control volume assumes the gas temperature, pressure and density are uniform within the cylinder and that stagnant conditions prevail. The energy and mass conservation principles yield:

$$\dot{m}_{\mathrm{in}} = \frac{\mathrm{d}m}{\mathrm{d}t} \tag{1}$$

$$\frac{\mathrm{d}U}{\mathrm{d}t} = \frac{\mathrm{d}(mu)}{\mathrm{d}t} = u\frac{\mathrm{d}m}{\mathrm{d}t} + m\frac{\mathrm{d}u}{\mathrm{d}t} = \dot{m}_{\mathrm{in}}h_{\mathrm{in}} - \dot{Q} \tag{2}$$

For our analysis we were interested in the increase in temperature and pressure over time. Due to the pressures achieved during filling, and the hydrogen compressibility at these high pressures (e.g., $Z = 1.23$ at 293 K and 350 bar) a real gas equation of state is required to determine the properties u and h_{in} as a function of temperature, pressure and specific volume [11]. Numerous equations of state exist for accurately predicting the properties of hydrogen in the range of temperature and pressure of interest. The Redlich–Kwong equation of state [2] was chosen for this analysis because it is accurate and computationally inexpensive. Eqs. (4) and (5) give the internal energy and enthalpy of the gas as a function of the temperature, pressure and specific volume:

$$p = \frac{R_{\mathrm{gas}}T}{v-b} - \frac{a}{T^{1/2}v(v+b)} \tag{3}$$

$$u = \frac{3a}{2bT^{1/2}}\ln\left(\frac{v}{v+b}\right) + u_0 \tag{4}$$

$$h = u - u_0 + pv - R_{\mathrm{gas}}T \tag{5}$$

The subscript 0 denotes the ideal gas value, a and b are constants for a specific gas. Substituting Eqs. (1) and (3)–(5) into Eq. (2) yields the equation for temperature rise of a real gas during re-fuelling:

$$\frac{\mathrm{d}T}{\mathrm{d}t} = \frac{\begin{array}{c}(\dot{m}_{\mathrm{in}}/m)(((R_{\mathrm{gas}}T_{\mathrm{in}}v_{\mathrm{in}})/(v_{\mathrm{in}}-b)) - (a/T_{\mathrm{in}}^{1/2}(v_{\mathrm{in}}+b)) \\ - R_{\mathrm{gas}}T_{\mathrm{in}} + T(C_p - C_v)) + (3a\dot{m}_{\mathrm{in}}/2m^2bT^{1/2}) \\ \times (m - (1/((1/m) + (b/V))) - (\dot{Q}/m)\end{array}}{(c_v - (3a/4bT^{3/2})\ \ln(1/(1+(bm/V))))} \tag{6}$$

As indicated, the rise in temperature is dependent on the temperature of the inlet gas T_{in}, the specific volume of the inlet gas v_{in}, the initial gas temperature T, the specific heat at constant pressure C_p and constant volume C_v, the internal volume of the cylinder V, the mass of gas within the cylinder at any point in time m, the rate of mass flow into the cylinder $\dot{m}$ and the rate of heat transfer to the cylinder walls, $\dot{Q}$.

Eq. (6) describes the physics that induce the temperature rise during filling. The difficulty in accurately predicting the temperature rise rests in determining the heat transfer to the cylinder wall. A detailed analysis of the heat transfer during filling is beyond the scope of the present study but it is the focus of ongoing research. In this work, Eq. (6) was solved for the case of an adiabatic fill ($\dot{Q} = 0$). This solution was used to calculate the adiabatic temperature rise. A fill where no heat from the gas is transferred to the cylinder walls represents a worst case scenario with the greatest increase in temperature.

3. Materials and experimental methods

There are many variables and operating parameters that affect the temperature field within the cylinder while filling (e.g., the mass flow rate and temperature of the gas entering the cylinder, the temperature of the cylinder walls, the ambient temperature, etc.). The hydrogen dispenser controls the rate of pressure rise within the cylinder, and in this manner, it controls the mass flow rate of hydrogen gas into the cylinder. The dispenser utilizes a pressure ramp rate (PRR) executed through a pressure control valve, which creates a large initial mass flow rate of hydrogen. This initial rate decreases steadily throughout the fill. The pressure ramp rate is adjustable but large ramp rates are limited by the flow restrictions inherent in the dispenser, hose and cylinder piping geometries.

In practical applications, the temperature of the gas entering the cylinder cannot be directly controlled. A typical fuelling station does not control the temperature of the gas within the large storage banks. The inlet temperature at the cylinder is affected by: (i) the initial temperature of the gas in the storage banks, (ii) the initial pressure of the storage banks, (iii) the hydrogen mass flow rate, (iv) the switching sequence of the storage banks, and (v) the ambient temperature during and prior to the experiment. The pressure ramp rate and the initial pressure of the cylinder are the two control variables used in the reported experiments.

3.1. Experimental test matrix

Three different pressure ramp rates were tested to determine the effect of the fill rate on the temperature field and temperature rise within the cylinder. The pressure ramp rates tested correspond to the nominal fill times of 40, 190, and 370 s (simulating fill times acceptable in hydrogen refuelling applications). The experimental fills were performed at initial pressures of 50, 75, 100, 150, and 200 bar (to simulate partially empty tanks at refuelling). The temperature of the hydrogen entering the cylinder was recorded but it was not controlled by the dispenser.

3.1.1. Repeatability

An initial set of tests were performed to investigate the repeatability of the temperature field measurements for a given set of control variables. These tests begin with the cylinder at 100 bar. The cylinder is filled to the rated mass of gas in 40 s. Several fills were carried out to investigate the repeatability of the inlet conditions provided by the dispenser and the temperature measurements within the cylinder.

Table 2
Experimental conditions

Fill time (s)	Initial pressure (bar)				
	50	70	100	150	200
Number of tests reported					
40	2	2	4	2	2
190	1		1		1
370	1		1		1

3.1.2. Effect of fill rate and initial pressure on temperature field

Fast fill experiments were performed for five different initial gas pressures within the cylinder, and three different nominal fill times. The aim of the experiment was to fill the cylinder to its rated mass capacity by monitoring the amount of gas transferred through the coriolis flow meter in the dispenser. The measurement was confirmed using our model predictions and the pressure and temperature measurements in the cylinder. The conditions for each test are outlined in the test matrix in Table 2.

3.2. Experimental setup

The experimental setup is shown schematically in Fig. 2. The fuelling station houses high pressure compressed gas inside ground storage banks. From these banks hydrogen is fed to the dispenser where it is metered and controlled. The dispenser is connected to the test cylinder by a 350 bar, quick connect fuelling nozzle. The test cylinder is instrumented with pressure sensors to monitor the tank pressure, a temperature sensor at the inlet to monitor the gas inlet temperature, and 63 temperature sensors inside the cylinder to record the gas temperature field. A detailed description of the main components of the test setup is described in the following sections.

3.2.1. Test cylinder

We used a type 3 aluminum lined, full carbon fiber wrapped cylinder for our experiments. The cylinder is manufactured by Dynetek Industries (model V074H350). It has an internal volume of 74 L and a design pressure of 350 bar (3.51 107 Pa). At 15 °C (288 K) this pressure rating translates into 1.79 kg of stored hydrogen. The relevant geometry and the experimental tank are illustrated in Figs. 2 and 3. The total inner length was 90 cm while the outer diameter was 40 cm. The cylinder is equipped with a 350 bar internal tank valve block assembly (Teleflex GFI model TV-115) which is also shown in Fig. 3. The assembly houses a 12 VDC solenoid valve, a manual shut-off valve, a pressure relief device, a pressure sensor mounted externally (PT) and a thermistor mounted internally (TT). The gas enters the cylinder through a stainless steel tube with a 5 mm internal diameter and extends 82 mm into the cylinder. The opposite end of the cylinder has a two-inch port, which is used as a sealed conduit for the thermocouple wires.

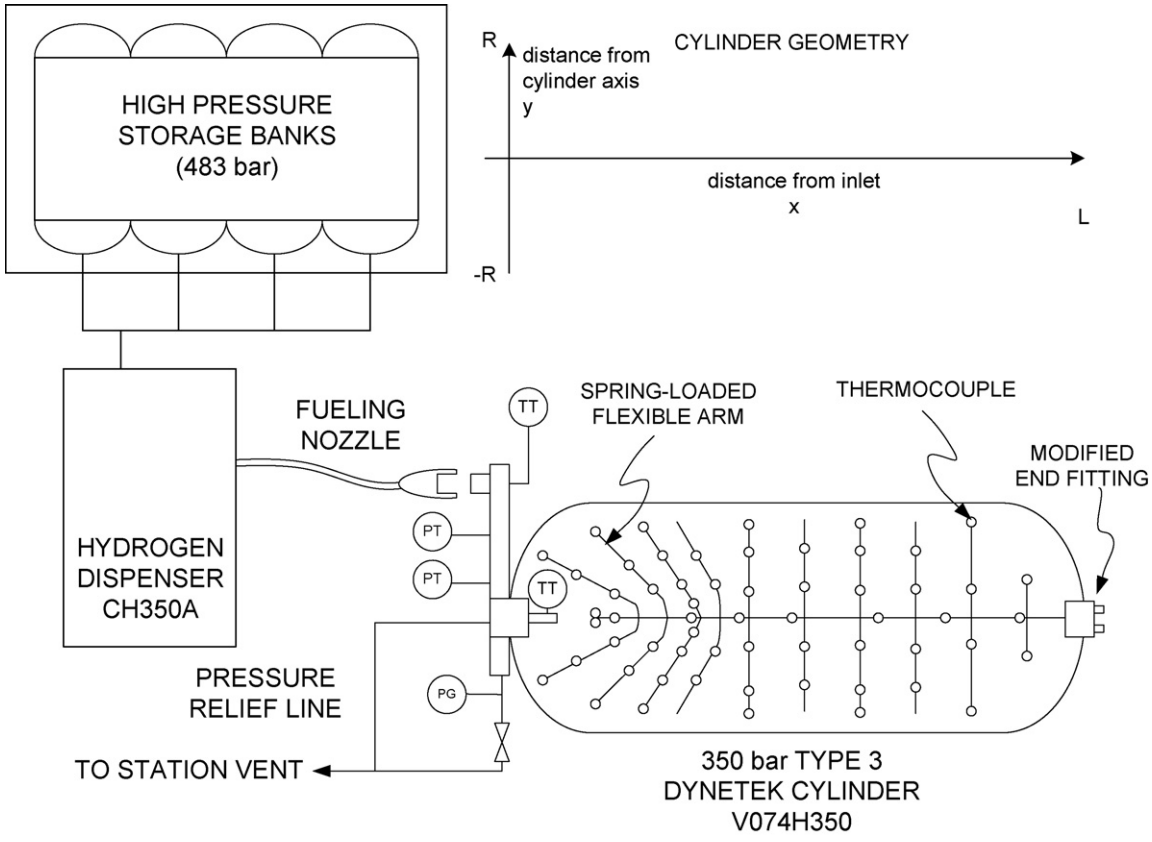

Fig. 2. Schematic of the test cylinder connection to the Fuelling Station.

3.2.2. Hydrogen dispenser

The Pacific Spirit Fuelling Station is equipped with a hydrogen dispenser designed and manufactured by General Hydrogen Corporation (model CH350A). This dispenser meters and controls the rate of filling, and it is equipped with a coriolis flow meter. With this sensor, the mass of hydrogen within the cylinder was known to within ±0.5% at all times during the fill. An electronically adjustable pressure control valve is used to set a pressure ramp rate of the gas entering the cylinder. The connection is made via a 1/4 turn quick-connect nozzle. The dispenser is capable of communication with the vehicle being fuelled in order to provide a faster and more accurate fill. An electrical interface to the tank allows the dispenser to monitor the pressure within the cylinder, provides a single temperature sensor signal from within the cylinder, and communicates the volume of the test cylinder. The volume of the cylinder is communi-

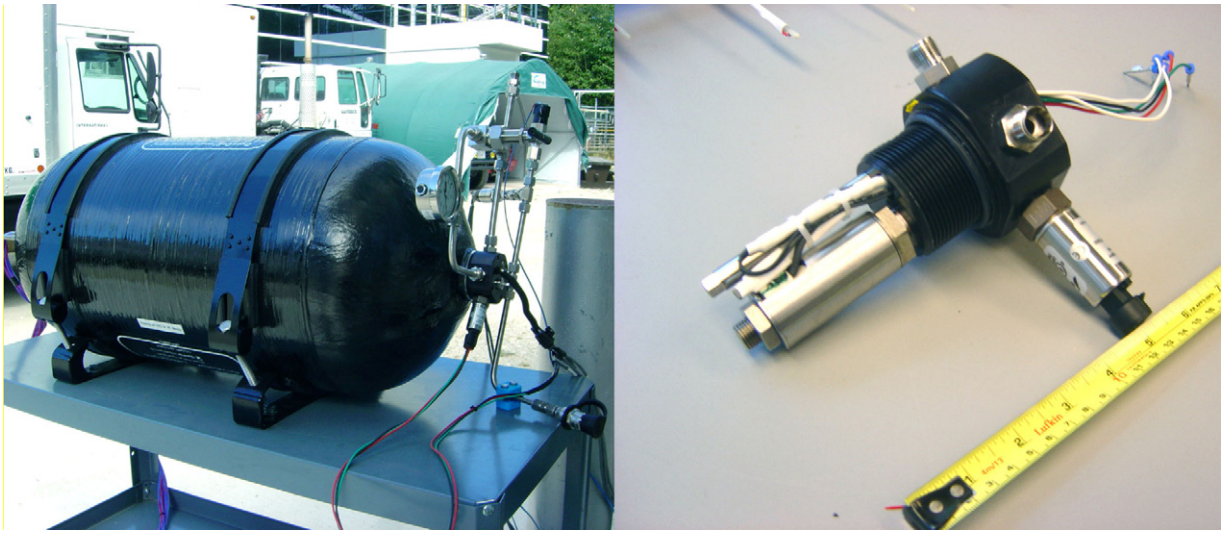

Fig. 3. Test cylinder with inlet and vent piping (left). Cylinder inlet valve block (right).

cated through a fixed resistor, where the value of the resistor is directly proportional to the volume of the cylinder. The communication protocols for the cylinder's pressure, temperature, and volume are specified in the SAE Standard J2601. This information enables accurate calculation of the initial mass of gas within the cylinder and the required mass of gas at the end of filling (based on the rated pressure, temperature and volume). The fixed communication link allows the dispenser to monitor the pressure and temperature of the gas in the cylinder throughout the fill to ensure the pressure does not exceed 1.25 times the design pressure and that the temperature of the gas does not exceed 358 K.

3.2.3. Instrumentation and data acquisition

The thermocouples used for measuring the temperature of the gas within the cylinder were type T (copper and constantan), bare wire, with a 0.5 mm tip diameter. These fine wire thermocouples have a response time of 0.40 s to achieve 63% of an instantaneous decrease in temperature from 427 to 38 °C when immersed in air moving at 60 ft s^{-1}. The thermocouples are accurate to within ±1 K. All sensors outputs were wired to a data acquisition system which recorded 63 internal gas temperatures, 20 surface temperatures, and the internal and inlet pressures. All signals were logged at 10 Hz.

3.2.4. Thermocouple locations and support mechanism

The thermocouples inserted into the gas cylinder are located in a grid arrangement to map out the temperature distribution. The thermocouples need to be held in position and that position must be known accurately to create plots of the temperature field. A major design constraint for the thermocouple mounting mechanism was related to the only access point (the end port which is two inches wide). The mechanism is shown in Fig. 4:

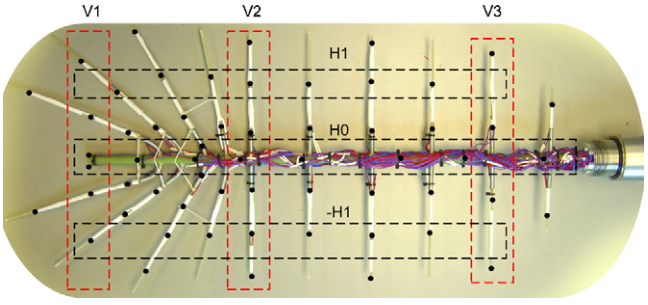

Fig. 4. Thermocouple support mechanism. The symbols indicate the sensor positions.

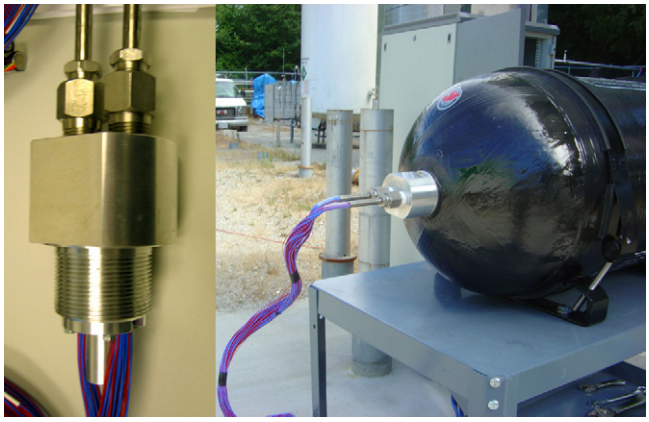

Fig. 5. Custom designed end fitting (left). Test cylinder during testing (right).

it incorporates a rigid base rod along the cylinder's centerline. Twenty thermocouple positioning arms were attached to this rod. The arms were in turn held in position by extension springs that allow the arms to be folded to insert or remove the mechanism from the cylinder. The main rod is mounted to the modified end plug in Fig. 3. In order to feed the electrical wires of the numerous thermocouples inside the cylinder, a custom designed end plug was fabricated. The end plug incorporates the same 2″—12 UN thread and o-ring seal as the OEM end plug, but also included 128 sealed wire conduits (see Fig. 5).

The areas delimited by the dashed lines in Fig. 4 correspond to vertical and horizontal slices cut through the plane of the thermocouple support mechanism inside the test cylinder. V1 is located at the inlet end of the cylinder while V3 is located at the opposite end. H1 is located in the top half of the cylinder, −H1 is located in the bottom half of the cylinder, etc. Table 3 gives the thermocouple coordinates for these areas.

4. Results

4.1. Repeatability

The electronic dispenser provided a reproducible mechanism to perform many fill simulations with the same initial and final conditions. For example, Fig. 6 shows the increase in temperature and pressure for three fills from a partially empty tank (100 bar nominal initial pressure), to the rated mass of gas of the cylinder (1.79 kg of H2) as measured by the dispenser. These and other experiments were used to corroborate the reproducibility of the pressure increase given the same preset pressure ramp

Table 3
Coordinates of thermocouples that make up slices V1, V2, V3, H1, H0, −H1

Vertical slices	Coordinates (x/L, y/R)	Horizontal slices	Coordinates (x/L, y/R)
V1	(0.2, −0.28) (0.19, −0.66) (0.2, 0.77) (0.21, 0.33) (0.2, 0.04) (0.2, −0.04)	H1	(0.11, 0.54) (0.26, 0.51) (0.35, 0.34) (0.32, 0.64) (0.4, 0.62) (0.45, 0.57) (0.55, 0.57) (0.64, 0.58) (0.74, 0.56) (0.93, 0.43)
V2	(0.45, −0.94) (0.45, −0.61) (0.45, −0.24) (0.46, 0.89) (0.45, 0.57) (0.45, 0.21) (0.44, 0)	H0	(0.2, 0.05) (0.28, 0) (0.68, −0.02) (0.44, 0) (0.54, −0.01) (0.36, −0.01) (0.79, 0) (0.92, −0.02)
V3	(0.86, −0.89) (0.85, −0.32) (0.83, 0.81) (0.84, 0.33)	−H1	(0.19, −0.66) (0.31, −0.63) (0.38, −0.63) (0.45, −0.61) (0.55, −0.60) (0.65, −0.63) (0.75, −0.61) (0.95, −0.51)

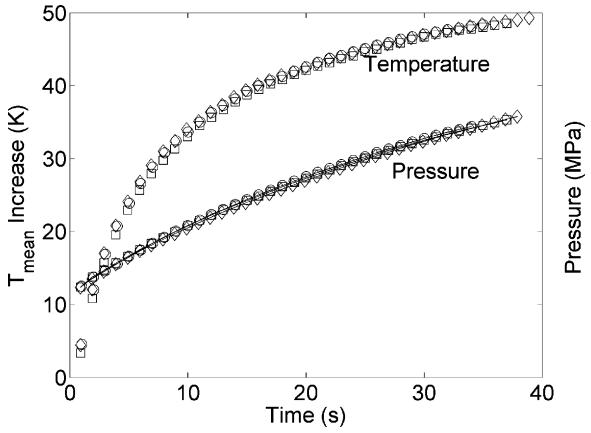

Fig. 6. The pressure and temperature rise curves were very reproducible for the same initial and final conditions. The plots show three representative data sets (from $P_i = 100$ bar to the rated capacity).

rate. The fills where completed on separate days with ambient temperatures in the range of 15–30 °C, to simulate real operating conditions for different climates. The results show that within this range of ambient temperatures, normalizing the results using the initial gas temperature accounts for the differences in environmental conditions.

4.2. Effect of initial pressure/mass of gas

Several fills were performed from nominal initial pressures of 50, 70, 100, 150, and 200 bar (i.e., ranging from 5×10^6 to 2×10^7 Pa). The experiments were automatically halted when the dispenser determined that the mass of gas within the cylinder had reached the rated capacity. The pressure ramp rate setting used during each fill were kept constant.

Fig. 7 shows the volume average temperature (T_{mean}) rise during the fill normalized by the initial temperature of the gas, for initial pressures of 50, 100 and 200 bar. The volume averaged temperature (hereinafter the mean temperature, T_{mean}) is calcu-

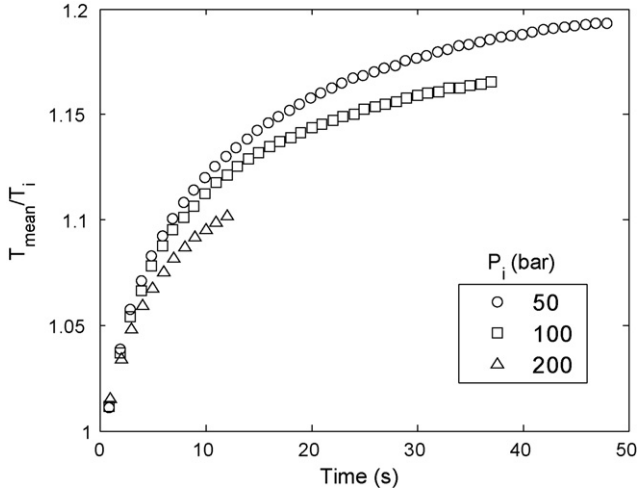

Fig. 7. The temperature rise during fills from 50, 100, and 200 bar to the rated capacity.

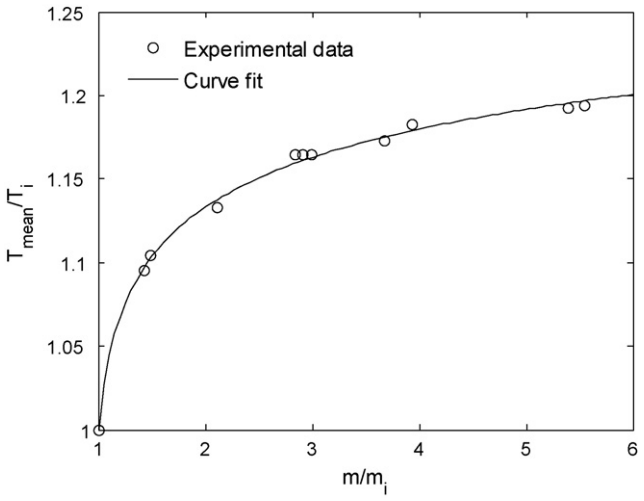

Fig. 8. The measured normalised mean temperature vs. the normalised mass. The curve fit can be obtained from Eq. (8).

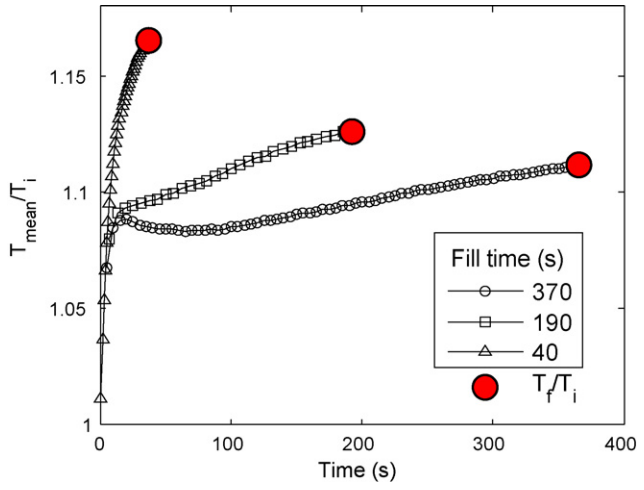

Fig. 9. The measured normalised temperature rise for three values of t_{total} ($m_f/m_i = 3$).

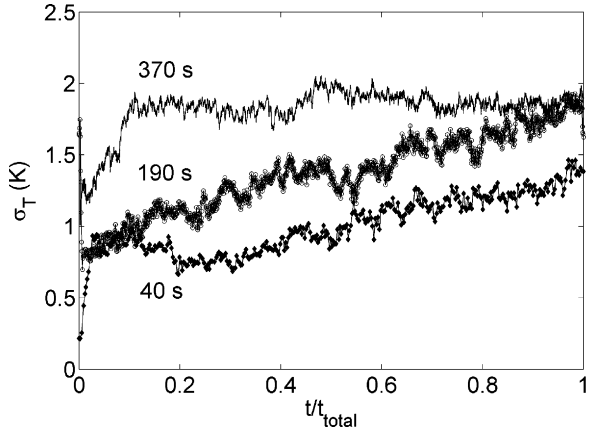

Fig. 10. The instantaneous standard deviation in temperature over three fills.

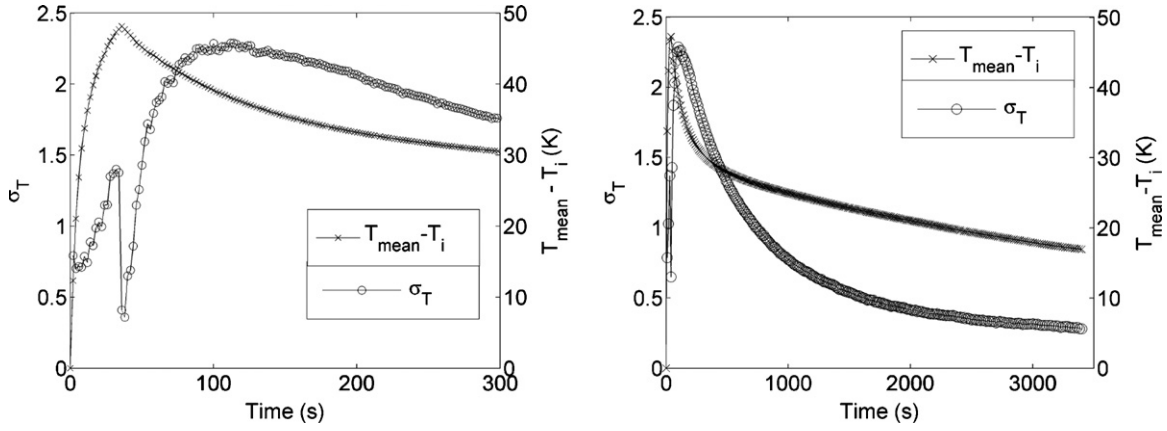

Fig. 11. Normalized mean temperature and instantaneous standard deviation during and after the fill (40 s) was completed.

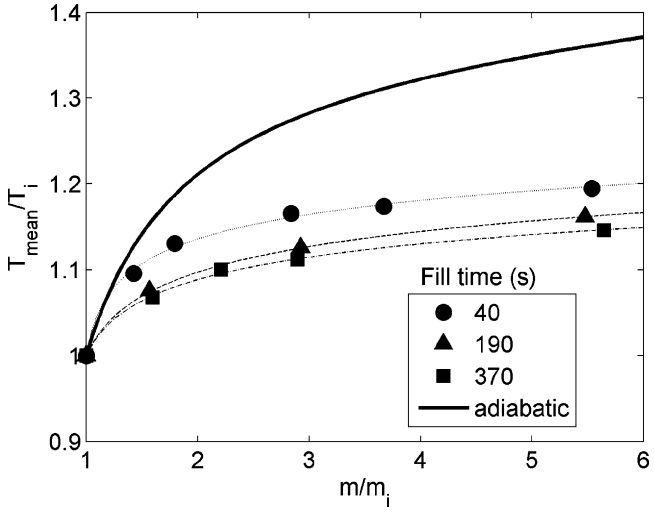

Fig. 12. The normalised temperature vs. the normalised mass increase for three fill rates. The solid line represents the temperature rise for a real gas under adiabatic conditions.

lated using Eq. (7). Where y_k is the absolute value of the vertical distance of the thermocouple to the centreline of the cylinder, T_k is the temperature reading of the thermocouple, and A_k is an area weighting given to each thermocouple:

$$T_{\text{mean}} = \frac{\sum_{k=1}^{63} y_k T_k A_k}{\sum_{k=1}^{63} y_k A_k} \tag{7}$$

All three curves show similar features: the greatest increase in temperatures occurs at the onset of filling and the rate of temperature increase gradually diminishes throughout the fill. The fill from 50 bar initial pressure shows the greatest increase in temperature while the fill from 200 bar shows the smallest increase in temperature. Hence, filling from a higher initial pressure yields a lower overall temperature rise. This is due to a greater amount (mass) of hydrogen dispensed when started from lower pressure. Since the dispenser is programmed with set pressure ramp rates, fills starting from higher pressures are shorter as less time is needed to achieve the desired amount of mass.

Hydrogen deviates from ideal-gas behaviour at high pressures. For this reason, our model used the Redlich–Kwong equation of state for hydrogen to calculate the initial and final mass of gas within the cylinder (from the experimental measurement of pressure and temperature). The use of the volumetric average of the 63 thermocouples within the cylinder provides a much more accurate assessment of the true average gas temperature than would be attained by a single temperature probe. The effect that initial mass within the cylinder has on the final temperature of the gas is illustrated in Fig. 8. The ratio of mean temperature to initial temperature is plotted against the ratio of final mass of gas to the initial mass of gas (the final mass is essentially the same for all fills). By normalizing both the temperature increase and the mass increase a trend is clearly shown. A point is included at the beginning of the fill (without dispensing any gas the temperature of the cylinder gas will remain the same). The relative increase in normalized temperature per unit

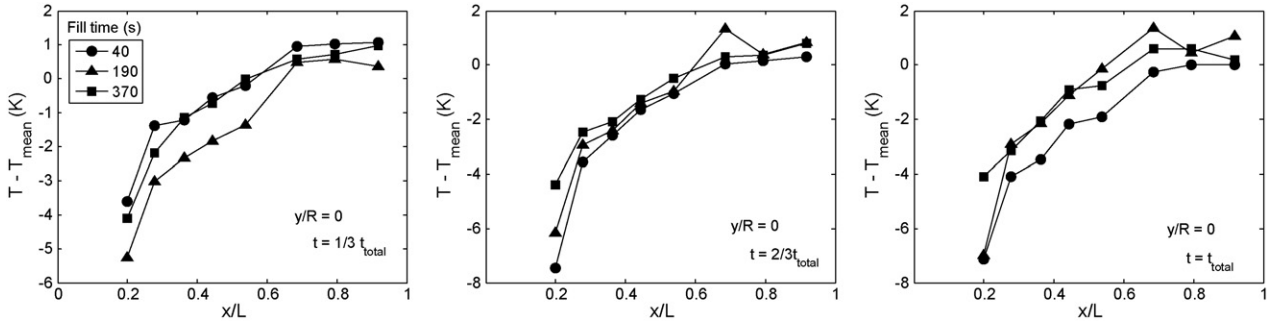

Fig. 13. The measured temperature along the cylinder axis for $t = t_{\text{total}}/3$, $2t_{\text{total}}/3$, and t_{total} (left, middle, right, respectively).

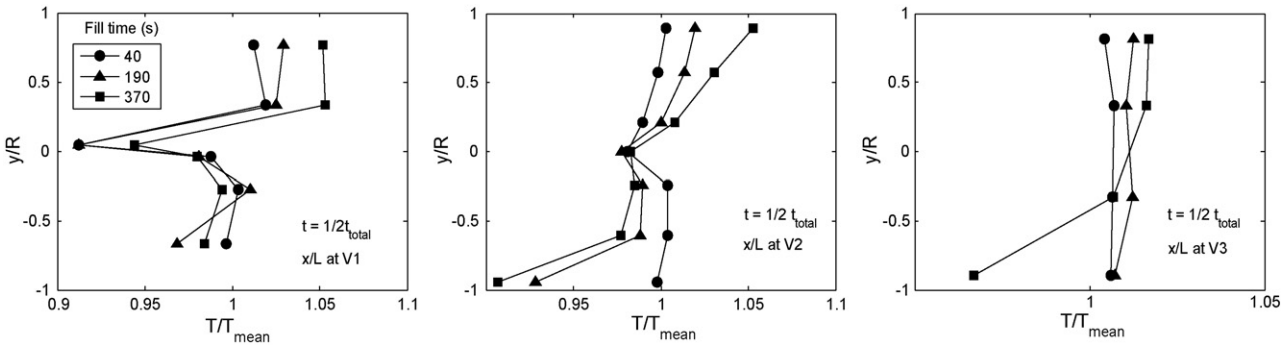

Fig. 14. The measured temperature along the vertical planes V1, V2, V3 (left, middle, right, respectively) at $t = t_{total}/2$ for three fills.

of normalized mass dispensed decreases as the amount of gas dispensed increases. The shape of the curve can be fitted to an expression of the form:

$$\frac{T_{mean}}{T_i} = \left(A + B\left(\frac{m}{m_i}\right)^{1/2} \right)^{C} \quad (8)$$

The observed curves are very similar to the shapes predicted by the analysis of Reynolds and Kays [6]. However, explaining the physical significance of the fitted parameters, or justifying the merits of a particular analytical model is beyond the scope of the present work. We only note that this type of empirical expressions can be useful to characterise cylinder designs. They could also be used in practical dispensing schemes based on temperature and pressure measurement only.

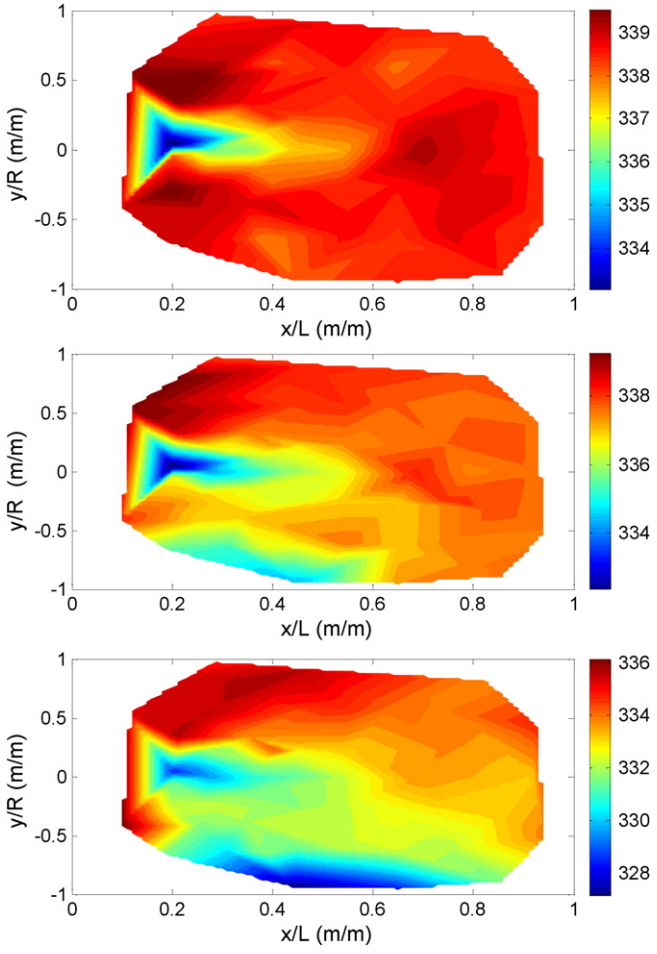

Fig. 15. The measured temperature distribution (in K) at $t = t_{total}/2$ for $t_{total} = 40$, 190, and 370 s (top, middle, bottom, respectively).

4.3. Effect of fill rate

Fig. 9 plots the normalized mean temperature throughout three fills with $t_{total} = 40$, 190 and 370 s. All three fills were initiated from a nominal initial pressure of 100 bar and were filled to the rated capacity of the cylinder yielding a ratio of final mass to initial mass of gas of 3.0. The large temperature rise at the beginning of filling is characteristic of a large initial mass flow rate of gas into the cylinder. This is an inherent characteristic of the dispenser design and geometry. After this initial rise in temperature, each fill proceeds at a separate pressure ramp rate leading to different overall fill times. The temperature rise is greatest for the short (40 s) fill and smallest for the long (370 s) fill. The lower final temperature of longer fill times is due to the increased amount of time for heat transfer between the gas and the cylinder wall. The effect of fill time is described by plotting the final temperatures versus the total fill time as indicated by the large circles in Fig. 9. Shorter fill times result in significantly higher final temperatures.

To quantify the temperature variation within the cylinder we calculated the standard deviation of the 63 temperatures (σ_T). Fig. 10 shows the calculated values for σ_T for three fills. All three fills have a ratio of final to initial mass of 3.0. In Fig. 10, the time coordinate is normalized as t/t_{total}, where t_{total} is the total time required to fill the cylinder.

The 40 s fill shows the lowest temperature variation and the greatest variation in temperature was observed during the 370 s fill. The results of Fig. 10 lead to the conclusion that longer fill times and hence lower mass flow rate into the cylinder results in a greater temperature variation within the cylinder. This is likely the result of temperature stratification in the cylinder due to buoyancy forces which are not negligible at low flow rates.

A lower mass flow rate results in a lower gas inlet velocity and hence a lower Froude number. For a 5-min fill from 100 bar to a settled pressure of 350 bar, the Froude number will approach unity near the end of the fill. At this point the effect of the inertial

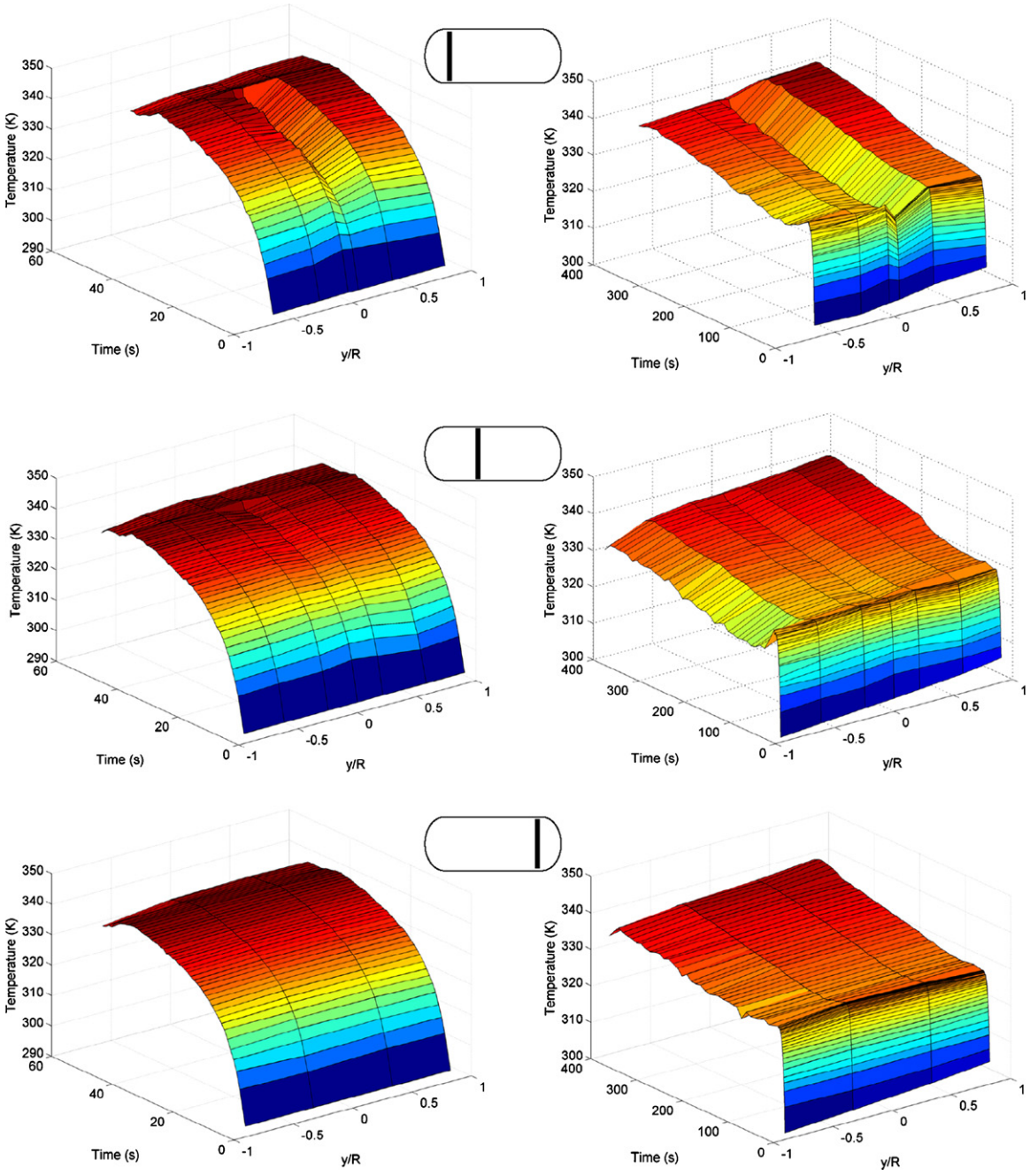

Fig. 16. The measured temperature distribution along three vertical slices (V1, V2, V3 correspond to top, middle, and bottom) during fast and slow fills. $t_{total} = 40$ and 370 s (for the left and right series, respectively).

forces, and the buoyancy forces on the velocity and temperature field within the cylinder become equivalent.

Fig. 11 shows the standard deviation of the 63 thermocouples and the normalized mean temperature for a 40 s fill from 100 to 350 bar. The standard deviation at the end of the fill dips down to a minimum and then quickly rises thereafter. This behaviour was attributed to the gas temperature at the in cylinder inlet rapidly approaching the mean temperature at the conclusion of filling. The increase thereafter is due to a greater temperature stratification as the temperature field is completely dominated by natural convection. The standard deviation reaches a maximum 1 min after the end of the fill and then decreases. The results on the right side of Fig. 11 indicate that the mean temperature of the gas decreases rapidly in the first 5 min after the end of the fill. Once the temperature difference between the gas and liner settles out, the rate of mean temperature change slows.

The overall effect of fill time and mass of gas dispensed is summarized in Fig. 12 and the relevant curve fitting parameters are summarised in Table 4. The normalized mean temperature is plotted against the normalized mass of gas (m/m_i) for three different fill times. In addition to the experimental measurements, Fig. 12 includes an equivalent plot for an adiabatic fill (the curve is the solution of Eq. (6) for the case $\dot{Q} = 0$). Slower fills result in a lower final gas temperature due to the additional time avail-

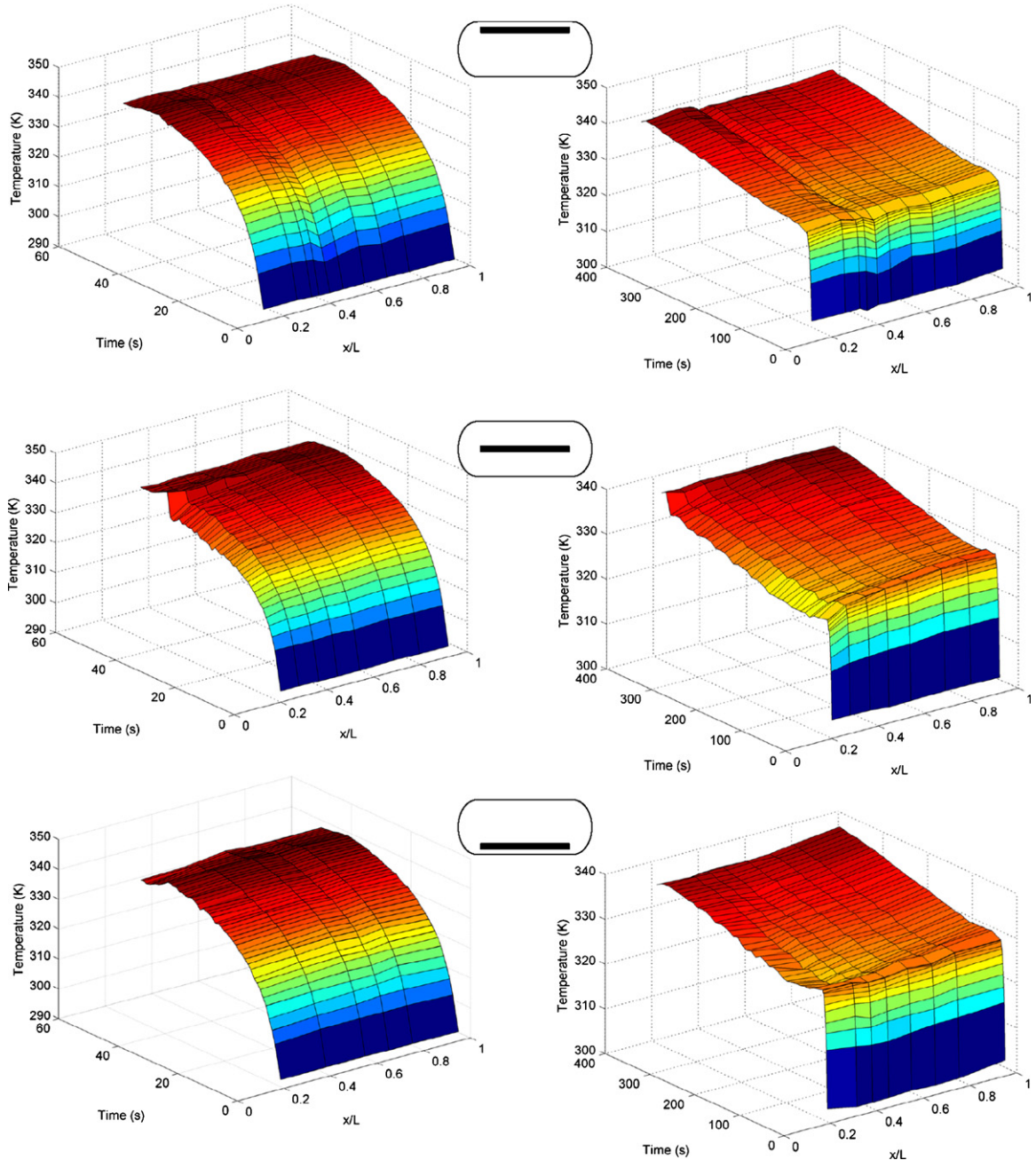

Fig. 17. The measured temperature distribution along three horizontal slices (H1, H0, −H1 correspond to top, middle, and bottom) during fast and slow fills. $t_{total} = 40$ and 370 s (for the left and right series, respectively).

able for the cylinder liner to absorb the heat of compression. For a fixed final mass, the lower the initial mass of gas the greater the final temperature will be, however, the greatest increase in temperature occurs with the initial increase in mass. The adiabatic temperature rise is independent of fill time because no heat is transferred in the process. The adiabatic fill represents the maximum temperature increase during a fill. The difference between the adiabatic fill and the 40, 190 and 370 s fills provides a direct indicator for the amount of heat generated (and ultimately transferred) to the cylinder.

Table 4
Curve fitting coefficients for the expression in Eq. (8)

Fill time (s)	*A*	*B*	*C*
40	−35.17000	36.16000	0.04595
190	−9.50400	10.50000	0.05526
370	−10.51000	11.50000	0.04841

The measured temperatures along the centreline normalized by the mean temperature at that point in time are shown in Fig. 13. The centreline temperature within the cylinder is important because it is the most accessible location for temperature measurements in practical applications with cylindrical fuel tanks. The measured temperature along the centerline increases

significantly from the inlet to the first thermocouple location. The lack of thermocouples in the first 15% of the length of the cylinder is due to the inlet tube which extents from the cylinder valve block approximately 10 cm into the cylinder as seen in Fig. 2. All three plots show a similar temperature profile with a rapid increase in temperature as the gas exits the inlet tube. The temperature increased from the inlet towards the opposite end where it approached the mean temperature. The temperature profile along the centerline has a similar shape in each of the three fills and throughout the duration of each fill.

Fig. 14 is a plot of the temperature profile in three vertical planes (V1, V2, V3). The temperature is normalized using the average temperature at the time of measurement. The distance from the centreline is normalized using the inner radius of the cylinder. The curves correspond to the instantaneous temperature at $t = t_{total}/2$ for three fill rates. These curves show a dip in temperature at the centreline as the jet of the cooler gas from the inlet is directed along the axis of the cylinder. The fastest fill shows the most uniform temperature in the top and bottom half of the cylinder. The 190 and 370 s fills show a vertical stratification of temperature. The degree of stratification increases with fill time as the slowest fill shows the greatest temperature variation in the vertical direction. This result shows that buoyancy will have a significant effect on the temperature distribution within the cylinder at longer fill times.

The overall temperature distributions at $t = t_{total}/2$ through the 40, 190 and 370 s fills are shown in Fig. 15. The greater mass flow rate into the cylinder which occurs during a shorter fills generated temperature distributions that were symmetric about the cylinder axis. For the slower fills, the temperature distribution became more and more stratified vertically due to lower gas velocities at the inlet (buoyancy forces became significant influence on the temperature field).

Two full temperature profile series along the three vertical slices in Fig. 3 (V1, V2, V3) are plotted in Fig. 16. The series on the left and right correspond to the shortest and longest total fuelling times ($t_{total} = 40$ and 370 s), respectively. For both fill rates, the temperature profiles along V1 show a significant dip in temperature at the cylinder centerline (due to the cool inlet gas). In all three planes, the long fill has a considerable temperature stratification when compared to its shorter counterpart. As previously noted, this is the result of the greater influence of buoyancy forces during the longer fill. Neglecting the dip in temperature along the centerline, the short fill shows a nearly uniform temperature in the vertical direction throughout the fill.

Similarly, the temperature profiles along the three horizontal slices in Fig. 3 (H1, H0, −H1) are plotted in Fig. 17. For the short fill the temperatures along H1 and −H1 are essentially uniform. The longer fill shows more temperature variation along slices H1 and −H1. Figs. 16 and 17 include data for $t = t_{total} + 10$ s. These data illustrate the temperature field that develops immediately after the conclusion of the fill. The figures show that the temperature near the inlet of the cylinder increases towards the mean gas temperature soon after the completion of the fill. The temperature field within the cylinder quickly begins to stratify after the flow of gas into the cylinder stops, and buoyancy drives the separation of the cooler gas to the bottom of the cylinder and the hotter gas to the top of the cylinder.

5. Conclusions

A 74 L type 3 compressed gas cylinder was instrumented with 63 thermocouples distributed along the vertical axial plane. These sensors were used to monitor and record the temperature field inside the cylinder during numerous experimental fills.

The cylinder was filled from initial pressures of 50, 70, 100, 150, and 200 bar to the rated capacity of the cylinder (1.79 kg of hydrogen) in order to assess the effect of the initial mass of gas on the temperature rise during filling. The greatest rate of temperature increase occurred at the onset of filling where the ratio of the current mass of gas to the initial mass of gas was the lowest. The rate of temperature rise decreases per amount of gas dispensed as the ratio of m/m_i increases.

The effect of fill rate was investigated by filling the cylinder from an initial pressure of 100 bar to the rated capacity of the cylinder at fill rates corresponding to total fill times of 40, 190, and 370 s. The faster fills generated larger temperature changes.

The effect of fill rate on the temperature distribution of the hydrogen gas within the cylinder was demonstrated by slower fills producing a temperature field with significant stratification in the vertical direction. This stratification was attributed to the greater influence of buoyancy forces at lower gas inlet velocities. The shorter fills produced a temperature field with a large conical temperature gradient extending out from the cylinder inlet and symmetrical about the cylinder axis.

The end opposite to the gas inlet experiences an instantaneous local temperature that best reflected the mean temperature of the gas. We suggest that this end is the optimal location for the temperature sensors aimed at fuel metering based on temperature and pressure measurements.

Acknowledgements

The authors would like to acknowledge General Hydrogen Corporation for their technical support and Western Economic Diversification Canada for the funding of this work and the projects associated with it. The authors would also like to thank Mark Rossetto of the National Research Council of Canada, Institute for Fuel Cell Innovation for his assistance in performing the experimental fills.

References

[1] ISO, Gaseous Hydrogen and Hydrogen Blends. Land Vehicle Fuel Tanks Part 1: General Requirements (ISO 15869). International Standard Organization, 2005.
[2] S. Charton, V. Blet, J.P. Corriou, Chem. Eng. Sci. 51 (2) (1996) 295–308.
[3] D.E. Daney, F.J. Edeskuty, M.A. Daugherty, Adv. Cryog. Eng. 41 (1996) 1041–1048.
[4] M.A. Haque, M. Richardson, G. Saville, Trans. IChemE 70 (Part B) (1992) 3–9.

[5] K. Kountz, W. Liss, C. Blazek, Proceedings of the 1998 International Gas Research Conference, 1998, pp. 135–145.
[6] W.C. Reynolds, W.M. Kays, Trans. ASME (1958) 1160–1168.
[7] J. Xia, Int. Comm. Heat Mass Transfer 20 (1993) 653–664.
[8] M.A. Haque, M. Richardson, G. Saville, Trans. IChemE 70 (Part B) (1992) 10–17.
[9] N. Newhouse, Fast filling of NGV fuel containers, SAE Technical Paper Series 1999-01-3739, 2005.
[10] J. Schneider, Fuel Cell Rev. 2 (4) (2005) 15–24.
[11] K. Annamalai, I.K. Puri, Advanced Thermodynamics Engineering, CRC Press, 2002.